Temperature-Dependent Magnetism

Unusual Magnetic Properties of the Edge-Sharing Bioctahedral Dirhenium(IV) Complex of Pyridine-2-thiolate**

Keisuke Umakoshi, Noriko Misasa, Chikako Ohtsu, Takashi Kojima, Maxim Sokolov, Makoto Wakeshima, Yukio Hinatsu, and Masayoshi Onishi**

Since the discovery of the $^3(\delta\delta^*)$ excited triplet state in a dimolybdenum(III) complex,[1] much effort has been devoted to the development of edge-sharing bioctahedral (ESBO) dimolybdenum(III) and ditungsten(III) complexes.[2] In ESBO complexes with a d^3–d^3 electron configuration, it is expected that the order of the molecular orbitals associated with metal–metal bonding is σ, π, δ*, δ, π*, and σ* in increasing in energy owing to mixing of the δ orbital with p orbitals on the bridging atoms.[3] The δ and δ* orbitals of diphosphine- or thiolato-bridged dimolybdenum and ditungsten complexes, however, are close in energy. The temperature-dependent magnetic properties of these complexes are consistent with the thermal population of the accessible excited triplet state.[1,2] Although several ESBO dirhenium(IV) complexes have also been synthesized to date, they are all diamagnetic.[4,5] Herein, we report the first μ-oxo-μ-thiolato ESBO dirhenium(IV) complex, which exhibits temperature-dependent magnetic properties that indicate the existence of a $^3(\delta\delta^*)$ excited state. We have also synthesized its one-electron reduced complex, and the structures and magnetic properties of Re_2^{IV} and $Re_2^{III,IV}$ complexes are compared.

It is known that the reaction of quadruply metal–metal-bonded dirhenium(III) complexes $(n\mathrm{Bu_4N})_2[\mathrm{Re_2X_8}]$ (X = Cl, Br) with pyridine-2-thiol (Hpyt) affords $[\mathrm{Re_2(pyt)_4X_2}]$ complexes that have a lantern structure with the retention of the metal–metal quadruple bond.[6] When the oxorhenium(V) complex $[\mathrm{ReOCl_3(PPh_3)_2}]$ was chosen as the starting material,

[*] Prof. Dr. K. Umakoshi, N. Misasa, C. Ohtsu, T. Kojima, Prof. Dr. M. Onishi
Department of Applied Chemistry
Faculty of Engineering
Nagasaki University
Bunkyo-machi, Nagasaki 852-8521 (Japan)
Fax: (+81) 95-819-2672
E-mail: kumks@net.nagasaki-u.ac.jp
onishi@net.nagasaki-u.ac.jp

Dr. M. Sokolov
Institute of Inorganic Chemistry
pr. Lavrentyeva 3, Novosibirsk 630090 (Russia)

Dr. M. Wakeshima, Prof. Dr. Y. Hinatsu
Division of Chemistry
Graduate School of Science
Hokkaido University
Kita-ku, Sapporo 060-0810 (Japan)

[**] This work was supported by a Grant-in-Aid for Scientific Research (No. 15550053) to K.U. We thank Mr. Eiji Yamaguchi and Miss Hikari Hamasaki for assistance.

Supporting information for this article is available on the WWW under http://www.angewandte.org or from the author.

  DOI: 10.1002/ange.200460532

the edge-sharing bioctahedral (ESBO) dirhenium(IV) complex $[Re_2Cl_2O(pyt)_4]$ (**1a**) with a Re_2OS framework was obtained as the major product.[7] The asymmetric structure of the neutral complex **1a** is shown in Figure 1a. The coordination environments of the two Re atoms are different; the Re1 atom is surrounded by a Cl_2N_2OS atom set, whereas the Re2 atom is surrounded by an NOS_4 atom set. The Re–Re distance and Re-S-Re and Re-O-Re angles are 2.5333(6) Å, 64.64(8)°, and 82.4(3)°, respectively. The metal–metal bond may be best described as a double bond (see below). It is noteworthy that the C–S distance (1.81(1) Å) in the pyt ligand containing the η^2-S atom is slightly longer than those (1.70(2)–1.74(1) Å) in the other three pyt ligands, which act as μ_2-S,N (η^1-S:η^1-N) bridges. It is also worth mentioning that the Re1–O1 and Re2–O1 distances differ considerably, whereas the Re1–S1 and Re2–S1 distances are comparable. A similar tendency was also observed for the minor isomer **1b**, though the Re1–O1 and Re2–O1 distances are much more similar in the one-electron reduced species, [PPN]-**2a** or $[Et_4N]$-**2a** (see below).

The structure of the linkage isomer (**1b**) obtained as the minor product is very similar to that of **1a** (Figure 1b).[7] The only difference in the structures of **1a** and **1b** is the direction of the pyt ligand chelating the Re2 atom; the N atom in the pyt ligand is *trans* to the bridging O atom in complex **1b**. The Re–Re distance and the Re-S-Re and Re-O-Re angles are 2.5419(6) Å, 64.44(7)°, and 82.8(3)°, respectively. The Re–S, Re–Cl, Re–N, and Re–O distances are very similar to those of **1a**.

The major isomer **1a** exhibits two reversible one-electron redox waves at −0.18 V ($Re_2^{III,IV}/Re_2^{IV}$) and +0.93 V ($Re_2^{IV}/Re_2^{IV,V}$) versus Ag/AgCl in CH_2Cl_2, indicating that the Re_2^{IV} state is stable in a wide potential range. The reduction of **1a** by hydrazine monohydrate in the presence of [PPN]Cl in CH_2Cl_2 under an argon atmosphere at ambient temperature afforded $[PPN][Re_2^{III,IV}Cl_2O(pyt)_4]$ ([PPN]-**2a**), which was crystallized by the diffusion of hexane vapor into the solution. The tetraethylammonium salt, $[Et_4N][Re_2^{III,IV}Cl_2O(pyt)_4]$ ($[Et_4N]$-**2a**), can also be obtained in a similar manner by using $[Et_4N]$Cl instead of [PPN]Cl. The X-ray structural analyses confirmed that both salts consist of a $[PPN]^+$ ion (Figure 2) or a $[Et_4N]^+$ ion and the complex anion in a 1:1 ratio.[7] The Re–Re distances in [PPN]-**2a** (2.5491(4) Å) and

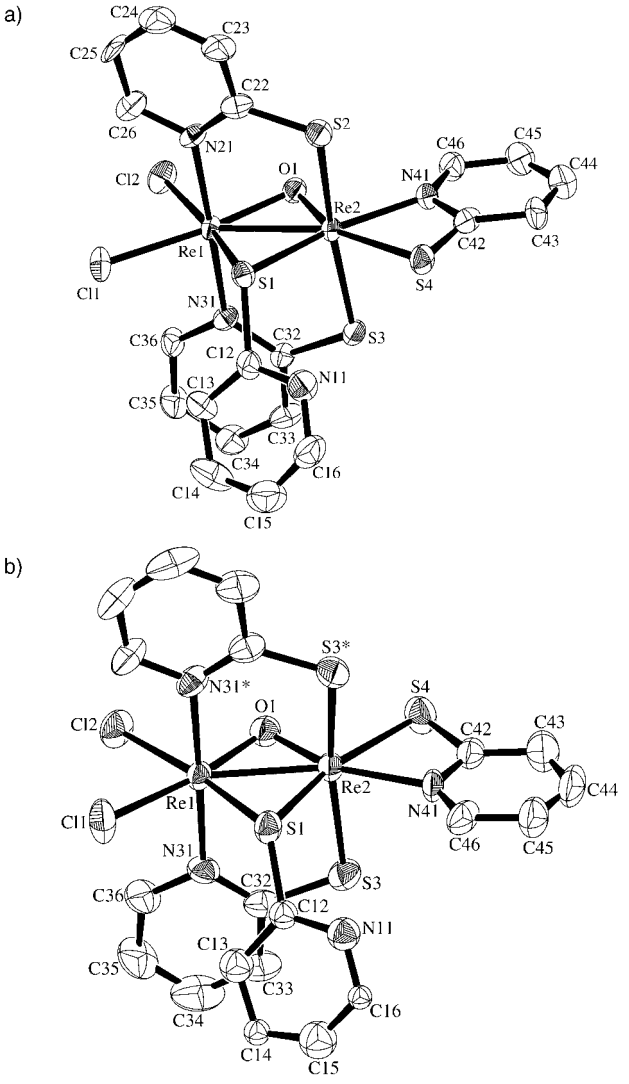

Figure 1. a) Molecular structure of the major isomer **1a** (50% probability ellipsoids). Selected bond lengths [Å] and angles [°]: Re1-Re2 2.5333(6), Re1-O1 1.977(9), Re1-S1 2.371(3), Re1-Cl1 2.390(3), Re1-Cl2 2.410(3), Re1-N21 2.16(1), Re1-N31 2.13(1), Re2-O1 1.868(8), Re2-S1 2.367(3), Re2-S2 2.358(4), Re2-S3 2.345(3), Re2-S4 2.450(3), Re2-N41 2.14(1); Re1-S1-Re2 64.64(8), Re1-O1-Re2 82.4(3). b) Molecular structure of the minor isomer **1b** (50% probability ellipsoids). Selected bond lengths [Å] and angles [°]: Re1-Re2 2.5419(6), Re1-O1 1.969(8), Re1-S1 2.366(3), Re1-Cl1 2.394(3), Re1-Cl2 2.413(3), Re1-N31 2.162(6), Re2-O1 1.872(7), Re2-S1 2.401(3), Re2-S3 2.337(2), Re2-S4 2.454(3), Re2-N41 2.148(8); Re1-S1-Re2 64.44(7), Re1-O1-Re2 82.8(3).

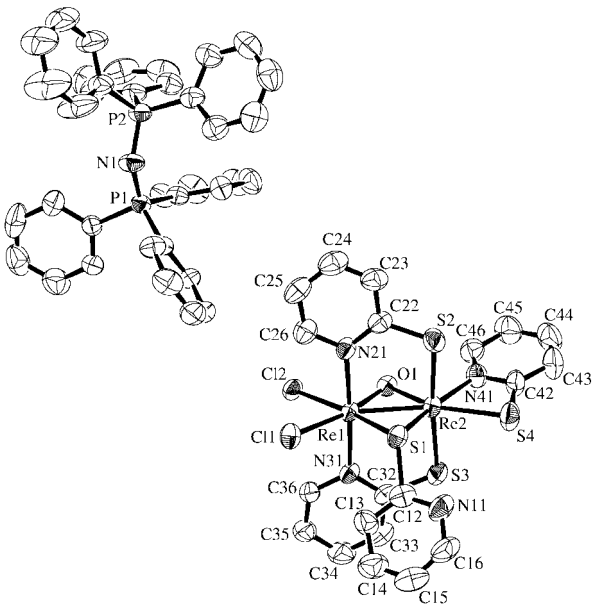

Figure 2. Molecular structure of $[PPN][Re_2Cl_2O(pyt)_4]$ ([PPN]-**2a**) (50% probability ellipsoids). Selected bond lengths [Å] and angles [°]: Re1-Re2 2.5491(4), Re1-O1 1.936(5), Re1-S1 2.362(2), Re1-Cl1 2.441(2), Re1-Cl2 2.431(2), Re1-N21 2.170(6), Re1-N31 2.153(6), Re2-O1 1.911(5), Re2-S1 2.359(2), Re2-S2 2.409(2), Re2-S3 2.379(2), Re2-S4 2.481(2), Re2-N41 2.132(7); Re1-S1-Re2, 65.36(5); Re1-O1-Re2, 83.0(2).

$[Et_4N]$-**2a** (2.5452(8) Å) have not changed significantly upon reduction from that in **1a** (2.5333(6) Å), which is in contrast to the case in which the Re–Re distance lengthens by 0.06 Å upon one-electron reduction of the ESBO dirhenium(IV) complex $[Re_2(\mu\text{-}O)_2(Metpa)_2](PF_6)_4$ (Metpa = [(6-methyl-2-pyridyl)methyl]bis(2-pyridylmethyl)amine).[5] Thus, the Re–Re distance in **1a** is relatively insensitive towards reduction. That the change in the number of electrons in δ and/or δ* orbitals by redox reaction has little influence on the metal–metal distance has also been reported for the oxidation (corresponding to the removal of an electron from δ* orbital) of some lantern-type dirhodium(II) complexes with an $\sigma^2\pi^4\delta^2\pi^{*4}\delta^{*2}$ electron configuration.[8]

The ^{1}H NMR spectra of Re_2^{IV} complexes **1a** and **1b** exhibit 16 distinct, sharp resonances between $\delta = +20$ and -40 ppm at 20 °C (see Figure S2 in the Supporting Information). As is the case for the complexes with a singlet ground state and those with a thermally accessible triplet excited state,[9] the ^{1}H NMR chemical shifts are temperature dependent (Figure 3). These observations prompted us to measure the

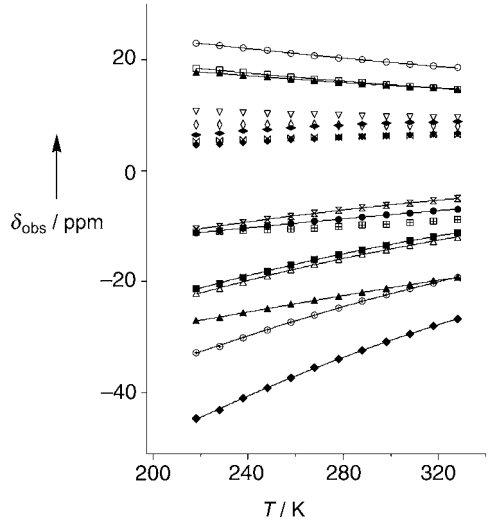

Figure 3. Temperature dependence of the proton chemical shifts in **1a**. All proton signals are derived from aromatic protons of pyridinethiolate ligands in different positions. The different symbols are experimental values; the solid lines are calculated from Equation (2) with the parameters listed in Table 1.

magnetic susceptibility of **1a** and its one-electron reduced species [PPN]-**2a** for comparison (Figure 4). Although the magnetic susceptibility data of [PPN]-**2a** indicate Curie–Weiss type magnetic behavior, the complex **1a** shows temperature-dependent behavior; the magnetic susceptibility (χ) increases with decreasing temperature and the curve tends to flatten below 100 K. A rapid increase of χ is observed below 20 K, which may be attributable to paramagnetic impurities. Cotton and co-workers reported the energy levels of d^3–d^3 dimers by fitting the van Vleck formula to the magnetic susceptibilities.[1,2] However, the χ–T curve of **1a**, which shows a constant paramagnetism below 100 K, does not obey their model. This constant contribution to χ can be accounted for by the van Vleck constant paramagnetism, and χ is given by

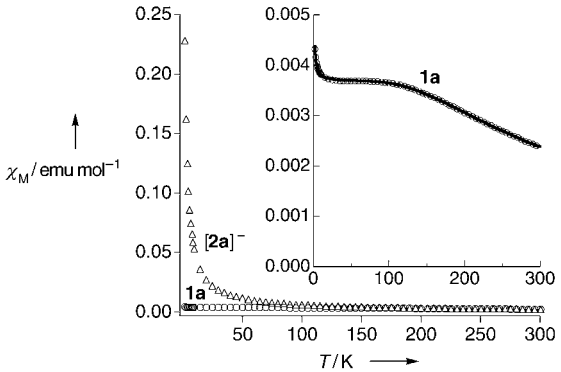

Figure 4. Plots of χ versus T for complexes **1a** (○) and [PPN]-**2a** (△) in the temperature range 2–300 K. Inset: Experimental values (○); the line is obtained from Equation (1) with the parameters listed in the text.

Equation (1), in which μ_B, E_1, and g_J are the Bohr magneton, the energy level of the first excited-state $^3B_{1u}$ ($J = 1$), and the Landé g factor, respectively, and α_0 (fixed to be 0) and α_1 is the constant derived from the van Vleck constant paramagnetism. The χ_{TIP} contribution to χ corresponds to a temperature-independent paramagnetism, and the nC/T accounts for the presence of small amounts of a paramagnetic impurity assumed to be a Re^{III} monomer with $S = 3/2$ in a proportion n. The best least-squares fit of Equation (1) to the susceptibility data leads to the following parameters: $g_J = 1.41(24)$, E_1 {$= E(^3B_{1u})$} $= 355(19)$ cm^{-1}, $\chi_{TIP} = 3.666(3) \times 10^{-3}$ emu mol^{-1}, $n = 0.075(1)$ %, $\alpha_1 = -0.0135(2)$ emu mol^{-1}.

$$\chi = (1-n)N\frac{\alpha_0 + \left\{\frac{2g_J^{\,2}\mu_B^{\,2}}{k_BT} + \alpha_1\right\}\exp\left(-\frac{E_1}{k_BT}\right)}{1+3\exp\left(-\frac{E_1}{k_BT}\right)} + \chi_{TIP} + n\frac{C}{T} \qquad (1)$$

The energy gap between the ground state and the triplet excited state can also be estimated by variable-temperature NMR studies.[9] The determination of the hyperfine coupling constant (A), the diamagnetic chemical shift (δ_{dia}) for the proton sites, the singlet–triplet energy separation (E_1), and the constant α_1 derived from the van Vleck constant paramagnetism, were initially attempted by a fit of the temperature dependence of the observed ^{1}H NMR chemical shifts, δ_{obs} (H_{obs}) to Equation (2), which also takes into account a contribution of the van Vleck constant paramagnetism.

$$H_{obs} = H_{dia} + \frac{H_0 A}{g_J\mu_B\gamma_H/2\pi}\bullet\frac{\left(\frac{2g_J^{\,2}\mu_B^{\,2}}{k_BT} + \alpha_1\right)\exp\left(-\frac{E_1}{k_BT}\right)}{1+3\exp\left(-\frac{E_1}{k_BT}\right)} \qquad (2)$$

However, we found that the hyperfine coupling constant A and the constant α_1 are strongly correlated, and the magnitude of these two parameters had a substantially smaller effect on the shape of the fitting curve as long as the product of the two parameters is almost constant. Because

it is difficult to determine A and α_1 a priori from the NMR data, the α_1 value was fixed to be $-0.0135\ \mathrm{emu\,mol^{-1}}$ as estimated from the susceptibility data. The g_J value was also fixed to be 1.41 in the curve fitting. The reliable parameters were obtained from 10 of the 16 resonances (Table 1). The

Table 1: Calculated magnetic and electronic parameters for **1a**.

Resonance	δ_{dia} [ppm]	A [MHz]	E_1 [cm^{-1}]
H1	27.1(4)	0.224(2)	314(19)
H2	22.5(4)	0.186(1)	277(21)
H3	20.9(3)	0.158(1)	301(20)
H9	−18.3(11)	−0.278(5)	215(31)
H10	−14.3(3)	−0.220(4)	367(19)
H12	−34.8(18)	−0.505(7)	227(30)
H13	−34.6(15)	−0.507(5)	249(27)
H14	−32.0(4)	−0.418(8)	397(16)
H15	−41.9(13)	−0.673(5)	289(21)
H16	−64.6(20)	−0.890(6)	270(22)

solid lines in Figure 3 show fitting curves obtained by using Equation (2) with the parameters listed in Table 1. Because the variable-temperature NMR data for the six remaining resonances could not be well fitted, probably due to the small change of H_{obs} in the range of temperature measured, the experimental data are plotted without fitting curves in Figure 3. The average S–T gap, E_1(av), estimated from the variable-temperature NMR studies is 291 cm^{-1}, and is thus very close to the value obtained from the susceptibility data.

These results indicate that the energy gap between the ground state and the triplet excited state in **1a** is smaller than those in diphosphine- or thiolato-bridged dimolybdenum(III) and ditungsten(III) complexes (Figure 5).[1,2] In this model, the

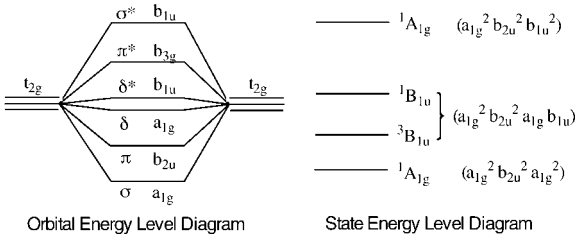

Figure 5. Qualitative orbital and state energy level diagrams for the case where $E(\delta) < E(\delta^*)$.

δ and δ* orbitals have very similar energies and the resulting $^3(\delta\delta^*)$ and $^1(\delta\delta^*)$ excited states are thermally accessible, though we could not estimate the energy level of the latter with sufficient reliability. The very close energies of the δ and δ* orbitals in **1a**, found for first time for an ESBO dirhenium(IV) system, may indicate that the metal–metal bond is best described as a double bond. The view is consistent with the description of the bond order for the diphosphine- or thiolato-bridged dimolybdenum(III) and ditungsten(III) complexes.[1,2]

In conclusion, a pair of ESBO dirhenium complexes in neighboring oxidation states, $[Re_2^{IV}Cl_2O(pyt)_4]$ and [PPN] $[Re_2^{III,IV}Cl_2O(pyt)_4]$, have been prepared. The X-ray structural analyses of these complexes revealed that the addition of an electron to the Re_2^{IV} complex does not influence the Re–Re distance in this system. Although the di-μ-oxo ESBO dirhenium complexes are diamagnetic, temperature-dependent magnetic behavior was observed for the μ-oxo-μ-thiolato Re_2^{IV} complex for the first time. The magnetic behavior of **1a** can essentially be understood by considering the model to be similar to those of diphosphine- or thiolato-bridged dimolybdenum(III) and ditungsten(III) complexes, though the van-Vleck constant paramagnetism should be taken into account probably due to the spin-orbit coupling in the third-row transition-metal ions.

Experimental Section

1a and 1b: A mixture of $[ReOCl_3(PPh_3)_2]$ (248 mg, 0.30 mmol) and pyridine-2-thiol (71 mg, 0.64 mmol) in 1,4-dioxane (100 mL) was refluxed for 12 h under an argon atmosphere. The dark brown solution was cooled to room temperature and filtered. The filtrate was concentrated to dryness.[10] The dark brown solid was dissolved in dichloromethane (15 mL) and precipitated again by addition of *n*-hexane (50 mL) into the solution. The precipitate was filtered, washed with diethyl ether, and dried in vacuo. Then about half of the solid was dissolved in dichloromethane, and the solution was loaded onto a silica gel column (40 × 3 cm) and eluted with dichloromethane. The second purple fraction (minor isomer, **1b**) and the third deep blue fraction (major isomer, **1a**) were collected and concentrated to dryness. The bluish-purple solid (**1b**) and the deep blue solid (**1a**) were washed with diethyl ether and then dried in vacuo. The same procedure of column chromatography was repeated again. Total yield of **1a**, 68 mg (51%); **1b**, 3 mg (2%). Crystals suitable for X-ray structural analysis were obtained by recrystallization from CH_2Cl_2 for **1a** and from CH_2Cl_2–CH_3CN for **1b**. Elemental analysis calcd (%) for $C_{20}H_{16}Cl_2N_4ORe_2S_4$: C 26.69, H, 1.79, N 6.23, S 14.25, Cl 7.88; found: **1a** [**1b**]: C 26.62 [26.84], H 1.72 [1.82], N 6.05 [6.35], S 14.53 [14.19], Cl 8.02 [7.84]; FAB-MS (*m*/*z*): 901 [*M*+H]; ^{1}H NMR (400 MHz, $CDCl_3$, 20 °C, TMS): **1a**: δ = 19.76 (d), 15.71 (t), 15.52 (d), 9.80 (dd), 8.44 (d), 8.15 (dd), 6.23 (2H), −6.46 (d), −8.17 (d), −9.72 (d), −13.87 (t), −14.69 (t), −21.60 (t), −22.99, −31.64 ppm; **1b**: δ = 19.93 (d), 17.30 (d), 15.92 (d), 15.14 (d), 14.97, 11.07 (d), 8.03 (dd), 5.69 (t), 2.08, 1.03, −10.70, −15.34, −17.54, −24.30, −28.13, −39.36 ppm.

[PPN]-2a: An excess amount of $N_2H_4{\cdot}H_2O$ (ca. 40 μL) was added to a solution of **1a** (161 mg, 0.18 mmol) and bis(triphenylphosphoranylidene)ammonium chloride ([PPN]Cl; 103 mg, 0.18 mmol) in dichloromethane (20 mL). The solution was stirred for 1 h at 20 °C under an argon atmosphere and filtered. To the filtrate was added *n*-hexane (2 mL) and the solution was left overnight. Brown crystals were collected, washed with *n*-hexane, and then dried in vacuo. Yield 211 mg (82%). Elemental analysis calcd (%) for $C_{56}H_{46}Cl_2N_5OP_2Re_2S_4$: C 46.76, H 3.22, N 4.87, S 8.91, Cl 4.93; found: C 46.69, H 3.39, N 5.03, S 9.25, Cl 4.88.

Received: May 1, 2004
Revised: October 8, 2004
Published online: December 13, 2004

Keywords: bridging ligands · magnetic properties · metal–metal interactions · mixed-valent compounds · rhenium

[1] F. A. Cotton, M. P. Diebold, C. J. O'Connor, G. L. Powell, *J. Am. Chem. Soc.* **1985**, *107*, 7438 – 7445.
[2] a) P. A. Agaskar, F. A. Cotton, K. R. Dunbar, L. R. Falvello, C. J. O'Connor, *Inorg. Chem.* **1987**, *26*, 4051 – 4057; b) F. A. Cotton, L. M. Daniels, K. R. Dunbar, L. R. Falvello, C. J. O'Connor, A. C. Price, *Inorg. Chem.* **1991**, *30*, 2509 – 2514; c) F. A. Cotton, J. L. Eglin, C. A. James, R. L. Luck, *Inorg. Chem.* **1992**, *31*, 5308 – 5315.
[3] a) S. Shaik, R. Hoffmann, C. R. Fisel, R. H. Summerville, *J. Am. Chem. Soc.* **1980**, *102*, 4555 – 4572; b) H. B. Bürgi, G. Anderegg, P. Bläuenstein, *Inorg. Chem.* **1981**, *20*, 3829 – 3834.
[4] a) G. Böhm, K. Wieghardt, B. Nuber, J. Weiss, *Inorg. Chem.* **1991**, *30*, 3464 – 3476; b) S. Ikari, T. Ito, W. McFarlane, M. Nasreldin, B.-L. Ooi, Y. Sasaki, A. G. Sykes, *J. Chem. Soc. Dalton Trans.* **1993**, 2621 – 2628.
[5] H. Sugimoto, M. Kamei, K. Umakoshi, Y. Sasaki, M. Suzuki, *Inorg. Chem.* **1996**, *35*, 7082 – 7088.
[6] R. M. Tylicki, W. Wu, P. E. Fanwick, R. A. Walton, *Inorg. Chem.* **1995**, *34*, 988 – 991.
[7] CCDC-236276, CCDC-236277, CCDC-236278, and CCDC-236279 contain the supplementary crystallographic data for this paper. These data can be obtained free of charge via www.ccdc.cam.ac.uk/conts/retrieving.html (or from the Cambridge Crystallographic Data Centre, 12, Union Road, Cambridge CB2 1EZ, UK; fax: (+44) 1223-336-033; or deposit@ccdc.cam.ac.uk).
[8] T. Kawamura, M. Maeda, M. Miyamoto, H. Usami, K. Imaeda, M. Ebihara, *J. Am. Chem. Soc.* **1998**, *120*, 8136 – 8142.
[9] a) G. C. Campbell, J. F. Haw, *Inorg. Chem.* **1988**, *27*, 3706 – 3709; b) F. A. Cotton, J. L. Eglin, B. Hong, C. A. James, *J. Am. Chem. Soc.* **1992**, *114*, 4915 – 4917; c) F. A. Cotton, H. Chen, L. M. Daniels, X. Feng, *J. Am. Chem. Soc.* **1992**, *114*, 8980 – 8983; d) C. Cremer, P. Burger, *J. Am. Chem. Soc.* **2003**, *125*, 7664 – 7677.
[10] The ^{1}H NMR spectrum of the hexane extract of the solid exhibits the signals of O=PPh_3 and PPh_3 in about a 1:2 ratio. The delay of the workup of the reaction mixture increases the amount of O=PPh_3 and thus the O=PPh_3/PPh_3 ratio. The reaction stoichiometry is $2\,[ReOCl_3(PPh_3)_2] + 4\,Hpyt \rightarrow [Re_2Cl_2O(pyt)_4] + O{=}PPh_3 + 3\,PPh_3 + 4\,HCl$. The triphenylphosphine ligand in the starting material acts as a reducing agent in the reaction.

